Drift of dark cavity solitons in a photonic-crystal fiber resonator

M. Tlidi,[1] L. Bahloul,[2] L. Cherbi,[2] A. Hariz,[2] and S. Coulibaly[3]
[1]*Faculté des Sciences, Université Libre de Bruxelles (U.L.B.), Campus Plaine CP 231, B-1050 Bruxelles, Belgium*
[2]*Laboratoire of Instrumentation, University of Sciences and Technology Houari Boumediene (USTHB), Algeria*
[3]*Université des Sciences et Technologies de Lille, Batiment P5, 59655 Villeneuve d'Ascq Cedex, France*
(Received 23 July 2013; published 4 September 2013)

We consider a photonic crystal fiber resonator pumped by a coherent injected beam. We show that temporal cavity solitons exhibit a motion with a constant velocity. This regular drift is induced by a broken reflection symmetry mediated by a third-order dispersion. We focus the analysis on dark temporal cavity solitons. They consist of asymmetric moving dips in a uniform background of the intensity profile. The number of the moving dips and their temporal distribution are determined solely by the initial conditions. We characterize this motion by computing the velocity of the dark temporal cavity soliton. Without fourth-order dispersion, dark cavity solitons do not exist.

DOI: 10.1103/PhysRevA.88.035802 PACS number(s): 42.81.Qb, 05.45.−a, 42.60.Da

A localized structure and localized patterns consist of one or more regions in one state surrounded by a region of a qualitatively different state. Such patterns may be stationary or oscillatory, static or moving (see overview on this issue [1,2]). They occur in various fields of nonlinear science, such as chemistry [3], plant ecology [4], and optics [5,6]. In all these systems, in spite of their diversity, localized structures and localized patterns are formed thanks to the balance between a positive feedback mechanism associated with chemical reaction or light matter interaction tending to amplify spatial inhomogeneities, and a diffusion or diffraction processes which on the contrary tends to restore spatial uniformity. In optics, they are often called cavity solitons and they are potentially interesting for the all-optical control of light. In addition, the system is far from thermodynamic equilibrium, exchanging permanently matter or energy with the environment. Localized structures can be created anywhere in the transverse plane. These solutions behave like particles. A fundamental property of localized structures is that several of them can coexist. The collision between them can lead to the annihilation of localized structure or the creation of a new one.

When using waveguides such as fibers, the diffraction or diffusion are neglected. In this case, the chromatic dispersion could play an important role. In particular, the interplay between dispersion and nonlinearity can lead to temporal modulation of continuous wave beams in all fiber resonators [7]. When diffraction and dispersion have a comparable influence on the system, 3D dissipative structures are formed. These structures consist of self-organized or isolated light bullets traveling at the speed of light within the resonator [8].

In fibers, localized structures often called temporal cavity solitons are nonlinear pulses that have been theoretically predicted [9] and experimentally observed in fiber ring resonators [10]. An estimation of the capacity to operate as all-optical memories is given: a very high value of 45 kbits at 25 Gbits/s [10]. Temporal cavity solitons are found in a well-defined region of parameters called a pinning zone. In this regime, the system exhibits a coexistence between two states: the homogeneous steady state (uniform background) and the periodic distribution of light that emerges from subcritical modulational instability [9,10]. When operating close to the zero dispersion wavelength [11,12], high-order chromatic dispersion effects could play an important role in the dynamics of photonic crystal fiber resonators, particularly in relation with supercontinuum generation [13,14]. Photonic crystal fibers permit a high control of the dispersion curve [12]. The inclusion of the fourth dispersion allows the modulational instability to have a finite domain of existence delimited by two pump power values [15]. This effect is also responsible for the stabilization of dark temporal cavity solitons (DTCSs) [16]. Recently, the link between temporal cavity soliton propagation [9,10] and frequency Kerr comb generation phenomenon in high-Q resonators [17] has motivated further the interest in this issue [18]. It has been shown that temporal cavity solitons circulating in the fiber cavity at the cavity repetition rate corresponds to a frequency comb in the spectral domain [18]. More recently, it has been shown in resonators without fourth-order dispersion that the third-order dispersion induces an asymmetry in the spectrum of periodic structures [19]. These studies are limited to fiber cavities with group-velocity dispersion restricted to the second and third orders.

In this paper, we study the combined effects of the third- and fourth-order dispersion on the stability of DTCSs in a photonic crystal resonator driven by a coherent beam. We show that the third-order dispersion induces a motion of DTCSs with a constant velocity. Moving dark temporal cavity solitons involved an asymmetric odd or even number of dips which coexist for finite values of the input field intensity. We estimate the velocity of asymmetric moving DTCSs.

We consider a photonic crystal fiber resonator pumped by a continuous wave of power S^2. A schematic setup of this device is depicted in Fig. 1. Assuming a single-mode optical fiber, the free propagation of light along the fiber is described by the nonlinear Schrödinger equation (NLS) in which the propagation constant is expanded up to the fourth order in a Taylor series. The NLS is supplemented by an appropriate coupling of mediated resonator boundary conditions. The extended NLS combined with boundary conditions leads to the generalized Lugiato-Lefever (LL) model. The generalized LL model can be nondimensionalized to [15]

$$\frac{\partial F}{\partial t} = S - (1 + i\Delta)F + i|F|^2 F + iB_2\frac{\partial^2 F}{\partial \tau^2} + B_3\frac{\partial^3 F}{\partial \tau^3} + iB_4\frac{\partial^4 F}{\partial \tau^4}, \quad (1)$$

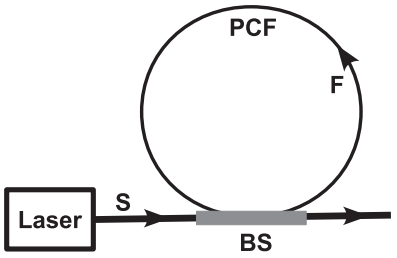

FIG. 1. Schematic setup of cavity filled with photonic crystal fiber (PCF) and driven by a coherent input beam S amplitude. BS denotes a beam splitter.

where F stands for the slowly varying envelope of the electric field circulating inside the cavity. The time t is the slow time scale used for describing the evolution of the field envelope F from one cavity round trip to the other. The coefficients $B_{2,3,4}$ account for the second-, third-, and the fourth-order chromatic dispersion, respectively. The time τ corresponds to the retarded time in the reference frame moving with the group velocity of the light. It is the fast time describing the variations of the structure of the field envelope resulting from the Kerr effect $i|F|^2F$, dispersion, and dissipation. The parameter Δ is the cavity detuning. The model of Eq. (1) is valid in the double limit of high cavity finesse, and the nonlinear cavity phase shift must be much smaller than unity. Furthermore, we assume that the length of the cavity is much shorter than the characteristic dispersion lengths of the field. In the range of injection levels that we consider, we can reasonably neglect the two-photon absorption and the Raman scattering by assuming that the nonlinearity time response of fiber is instantaneous. More precisely, when pulse width is larger than 1 ps, the Kerr effect becomes dominant and therefore these two effects could be ignored [20]. Finally, we assume that the optical field maintains its polarization as it propagates along the fiber. We therefore neglect polarization instabilities.

The homogeneous steady states (HSSs) of Eq. (1) satisfy $S = [1 + i(\Delta - |F_s|^2)]F_s$. These solutions are not affected by the high dispersion effects. They are identical to the LL model [21]. We consider the bistable regime where $\Delta > \sqrt{3}$ and we perform the linear stability analysis of the HSS with respect to finite frequency perturbations of the form $\exp(i\omega\tau + \lambda t)$. This analysis yields eigenvalues of the linear operator

$$\lambda = -1 + iB_3\omega^3 \pm \sqrt{I_s^2 - (\Delta - 2I_s + B_2\omega^2 - B_4\omega^4)^2},$$

where $I_s = |F_s|^2$ corresponds to the uniform intensity background of light. The HSSs undergo two modulational instabilities at thresholds $I_{m1} = 1$ and $I_{m2} = [2[B_2/(4B_4) + \Delta] + \sqrt{\{B_2/(4B_4) + \Delta]^2 - 3\}}/3$. The second modulational instability is induced by the fourth-order dispersion and allows restabilization of the HSS for $I_s > I_{m2}$. At this second modulational instability threshold, the critical frequency is $\Omega_{m2}^2 = B_2/(4B_4)$. The corresponding critical injected field intensity is $S_{m2}^2 = I_{m2}[1 + (\Delta - I_{m2})^2]$. In the linear regime, the critical frequency as well as the threshold associated with modulational instability are not affected by the third-order dispersion. The linear velocity of the periodic train of dips is

$$v_l = \frac{\partial I_m(\lambda)}{\partial\omega} = \frac{3B_2B_3}{4B_4}. \tag{2}$$

To calculate the nonlinear solutions bifurcating from the threshed associated with modulational instability, we use a weakly nonlinear analysis. To this end we decompose the electric field F into its real and imaginary parts, and we expand the field F and the input field amplitude S in terms of a small parameter μ that measures the distance from the modulational instability threshold. The third order adds a new phase in the dynamics of all fiber cavities. This phase is equal to $-B_3\Omega_{m2}^3$. At third order in μ, the solvability conditions yield the following amplitude equation: $\partial A/\partial t = \alpha A + (h_1 + ih_2)|A|^2 A$, where $\alpha = S^2 - S_{m2}^2$ measures the distance from the second instability threshold. The coefficient h_2 proportional to the the new phase $-B_3\Omega_{m2}^3$. In the case where $B_3 = 0$, the coefficient of the cubic term in this equation is real, i.e., $h_2 = 0$. Assuming that the solution of this amplitude equation has the form $A = R\exp(iqt)$, the stationary solutions are $R = \pm\sqrt{-\alpha/h_1}$ and the phase $q = -h_2\alpha/h_1$. The velocity of the periodic train of dips is

$$v = \frac{3B_2B_3}{4B_4} - \frac{4B_4h_2\alpha}{B_2h_1}. \tag{3}$$

The velocity of periodic solutions is corrected by the presence of a new phase q which is proportional to the distance α from the critical point associated with the second modulational instability (I_{m2}, S_{m2}). Weakly nonlinear analysis in the neighborhood of this threshold allows us to determine the condition under which modulational instability appears subcritically. This transition from supercritical to subcritical bifurcation requires that $h_1 = 0$. This condition corresponds to the threshold associated with the formation of DTCS. Normal form or amplitude equations describing the temporal evolution of slow unstable modes in the neighborhood of the modulational instability cannot support dissipative temporal cavity solitons. The weakly nonlinear theory, although, gives information about the threshold associated with the appearance of DTCS but cannot describes DTCS because it does not take into account the nonadiabatic effects that involve the fast temporal scales which are responsible for the stabilization of DTCS [22]. However, the inclusion of amended terms can catch this type of dynamics [23].

The formation of a periodic train of dips that emerge from a subcritical modulational instability is often the prerequisite condition for the formation of temporal cavity solitons [9,10]. In free propagation, it has been shown that the nonlinear Schrödinger equation admits an exact solution in the form of a bright soliton in the anomalous dispersion region of the fiber and dark solitons in the normal dispersion regime [24]. This theoretical prediction was confirmed by experiments [25,26]. In what follows we will focus our analysis on the temporal cavity solitons. Direct numerical simulations of Eq. (1) with periodic boundary conditions close the second threshold show a motion of both bright and dark temporal cavity solitons, as shown in Fig. 2. The inclusion of the third-order description renders the profile of cavity solitons asymmetric, as shown in Fig. 2. This asymmetry originates from the

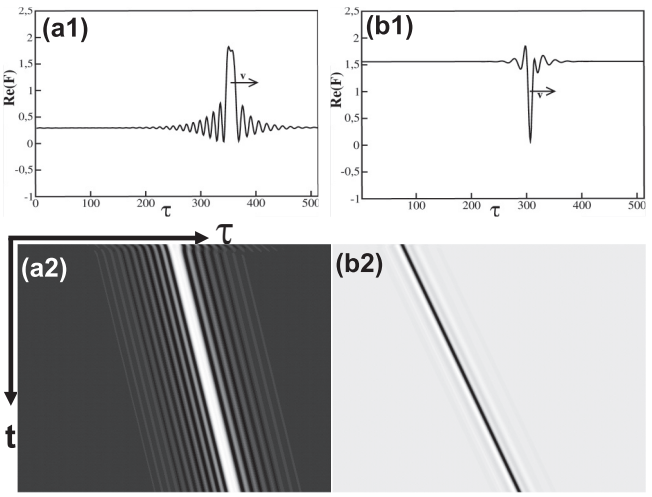

FIG. 2. Single moving (a1) bright and (b1) dark temporal cavity solitons obtained by numerical simulations of Eq. (1). The parameters are $B_2 = 0.75$, $B_3 = 0.12$, $B_4 = 0.2$, and $\Delta = 3$. For (a1, a2) $S = 2$; (b1, b2) $S = 2.4$; and (a2, b2) are $\tau - t$ maps showing the time evolution of bright and dark cavity solitons, respectively. Maxima are plain white and mesh number integration is 512.

third-order dispersion term in Eq. (1) that breaks the reflection symmetry ($\tau \to -\tau$). This asymmetry breaking occurs also in synchronization mismatch, i.e., the difference between the laser repetition time and the cavity round-trip time [27]. This effect leads to convection in the fiber cavity through pumping synchronization mismatch due to inaccuracy in the cavity length.

In what follows, we focus on DTCS. A bifurcation diagram of a single moving DTCS that emerges from the modulational instability located at the point S_{m2} is shown in Fig. 3. We plot in this figure only a portion of the upper HSS solution. From the threshold S_{m2} emerges an unstable branch of moving DTCS subcritically. The full lines indicate the minimum values of the real part of the intracavity field associated with DTCS.

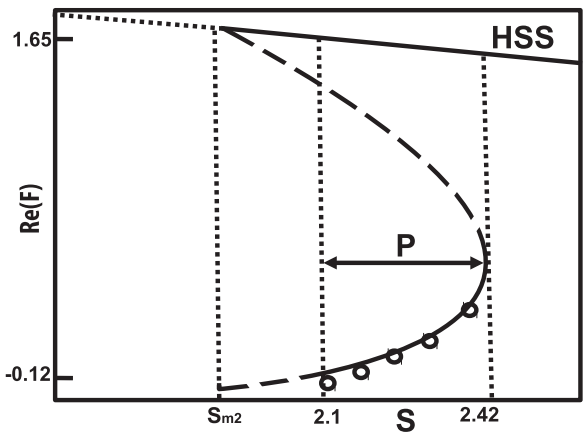

FIG. 3. Bifurcation diagram associated with a moving single dark temporal cavity soliton. Parameters are $B_2 = 0.75$, $B_3 = 0.12$, $B_4 = 0.2$, and $\Delta = 3$. The full (broken) curve indicates stable (unstable) solutions. The open circle indicates the minimum numerical values of the real part associated with moving DTCS.

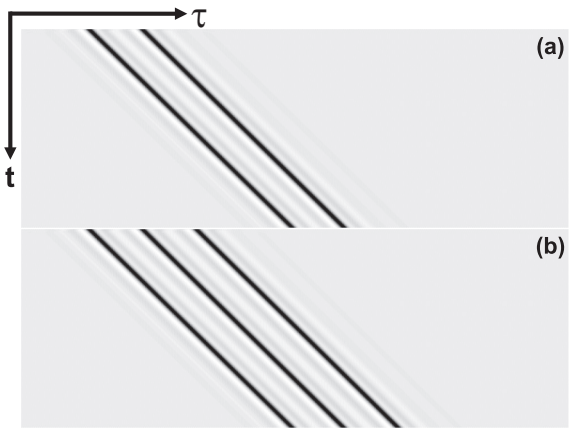

FIG. 4. $\tau - t$ maps showing the time evolution dark cavity solitons obtained for the same parameters as in Fig. 2(b), the real part of the intracavity field presenting (a) two and (b) three moving dark temporal solitons obtained by numerical simulations of Eq. (1).

The corresponding numerical values are indicated by open circles. At the turning point $S_l \approx 2.42$, the DTCS becomes stable. When decreasing the input field amplitude, a coexisting behavior between the HSS and DTCS occurs in the range $S_{m2} < S < S_l$. Inside this hysteresis loop, there exists a region of the S parameter values called a pinning zone P where moving DTCS occurs. In this regime, Eq. (1) admits a set of moving DTCSs that exhibit $2n + 1$ or $2n$ moving dips, where n is a positive integer. The limit $n \to \infty$ corresponds to the infinitely extended, moving periodic train of dips. Examples of moving DTCS having different numbers of dips are illustrated in Fig. 4. The number of dips and their temporal distribution depend on the initial conditions used. They are obtained for the same parameter values as in Fig. 3 and differ only by the initial condition. The velocity of the moving DTCS is affected by correction to the velocity provided by the linear analysis [cf. Eq. (3)], namely, $v = v_l + v_{nl}$. From the parameter values of Fig. 2(b1), analytical and numerical simulations of Eq. (1) show that $S_c \approx S_{m2}$. The velocity obtained from the linear stability analysis $v_l \approx 0.34$, and that obtained from the numerical simulations is $v_{\text{num}} \approx 0.27$. The difference between the two velocities corresponds to the nonlinear correction. The velocity should depend on the distance from the threshold.

In conclusion, we have identified dynamical behavior due to the third-order dispersion in an all-fiber resonator driven by a coherent radiation beam, i.e., motion of a dark temporal cavity soliton with a constant velocity. We characterized the motion by constructing the bifurcation diagram associated with the motion of a single dark temporal cavity soliton and we estimate the velocity.

M.T. received support from the Fonds National de la Recherche Scientifique (Belgium). This research was supported by the Interuniversity Attraction Poles program of the Belgian Science Policy Office, under Grant IAP P7-35.

[1] V. S. Zykov, *Simulation of Wave Processes in Excitable Media* (Manchester University Press, Manchester, UK, 1987); D. Mihalache *et al*., Prog. Opt. **27**, 229 (1989); J. D. Murray, *Mathematical Biology*, 3rd ed. (Springer, Berlin, 2003); Y. S. Kivshar and G. P. Agrawal, *Optical Solitons: From Fiber to Photonic Crystals* (Academic, New York, 2003); P. Mandel and M. Tlidi, J. Opt. B **6**, R60 (2004); A. S. Mikhailov and K. Showalter, Phys. Rep. **425**, 79 (2006); L. Pismen, *Vortices in Nonlinear Fields: From Liquid Crystals to Superfluids, From Non-Equilibrium Patterns to Cosmic Strings* (Clarendon Press, Oxford, 1999); H.-G. Purwins, H. U. Bödeker, and Sh. Amiranashvili, Adv. Phys. **59**, 485 (2010).

[2] K. Staliunas and V. J. Sanchez-Morcillo, *Transverse Patterns in Nonlinear Optical Resonators*, Springer Tracts in Modern Physics Vol. 183 (Springer Verlag, Berlin, 2003); A. Malomed *et al*., J. Opt. B **7**, R53 (2005); M. Tlidi *et al*., Chaos **17**, 037101 (2007); N. Akhmediev and A. Ankiewicz, *Dissipative Solitons: From Optics to Biology and Medicine* (Springer-Verlag, Berlin, 2008); O. Descalzi, M. Clerc, S. Residori, and G. Assanto, *Localized States in Physics: Solitons and Patterns* (Springer, New York, 2011); M. Peckus, R. Rogalskis, V. Sirutkaitis, and K. Staliunas, Lith. J. Phys. **53**, 25 (2013)

[3] S. Koga and Y. Kuramoto, Prog. Theor. Phys. **63**, 106 (1980); L. Yu. Glebsky and L. M. Lerman, Int. J. Nonlion. Sci. **5**, 424 (1995); A. R. Campneys, Physica D **112**, 158 (1998); G. W. Hunt, G. J. Lord, and A. R. Champneys, Compt. Methods Appl. Mech. Eng. **170**, 239 (1999); P. Coullet, C. Riera, and C. Tresser, Phys. Rev. Lett. **84**, 3069 (2000); V. K. Vanag *et al*., Nature (London) **406**, 389 (2000); I. Lengyel and I. R. Epstein, Proc. Natl. Acad. Sci. USA **89**, 3977 (1992); V. K. Vanag and I. R. Epstein, Phys. Rev. Lett. **92**, 128301 (2004); M. G. Clerc, A. Petrossian, and S. Residori, Phys. Rev. E **71**, 015205 (2005); V. S. Zykov and K. Showalter, Phys. Rev. Lett. **94**, 068302 (2005); T. Kolokolnikov and M. Tlidi, *ibid*. **98**, 188303 (2007); M. Tlidi, G. Sonnino, and M. Bachir, Phys. Rev. E **86**, 045103 (2012).

[4] O. Lejeune, M. Tlidi, and P. Couteron, Phys. Rev. E **66**, 010901(R) (2002); E. Meron *et al*., Chaos Solitions Fractals **19**, 367 (2004); M. Rietkerk *et al*., Science **305**, 1926 (2004); E. Meron *et al*., Chaos **17**, 037109 (2007); M. Tlidi, R. Lefever, and A. G. Vladimirov, Lect. Notes Phys. **751**, 381 (2008); E. Sheffer *et al*., J. Theor. Biol. **273**, 138 (2011); W. R. Tschinkel, PLoS ONE **7**, e38056 (2012); M. D. Cramer and N. N. Barger, *ibid*. **8**, e70876 (2013).

[5] M. Tlidi, P. Mandel, and R. Lefever, Phys. Rev. Lett. **73**, 640 (1994); M. Tlidi *et al*., Opt. Lett. **25**, 487 (2000); A. J. Scroggie, J. M. McSloy, and W. J. Firth, Phys. Rev. E **66**, 036607 (2002); O. A. Egorov, F. Lederer, and Y. S. Kivshar, Opt. Express **15**, 4149 (2007); L. Gelens *et al*., Phys. Rev. A **75**, 063812 (2007); A. G. Vladimirov *et al*., Opt. Express **14**, 1 (2006); O. A. Egorov, F. Lederer, and K. Staliunas, Phys. Rev. A **82**, 043830 (2010); A. G. Vladimirov, R. Lefever, and M. Tlidi, *ibid*. **84**, 043848 (2011).

[6] V. B. Taranenko, K. Staliunas, and C. O. Weiss, Phys. Rev. A **56**, 1582 (1997); G. Slekys, K. Staliunas, and C. O. Weiss, Opt. Commun. **149**, 113 (1998); V. B. Taranenko, K. Staliunas, and C. O. Weiss, Phys. Rev. Lett. **81**, 2236 (1998); S. Barland *et al*., Nature (London) **419**, 699 (2002); X. Hachair *et al*., Phys. Rev. A **72**, 013815 (2005); X. Hachair, G. Tissoni, H. Thienpont, and K. Panajotov, *ibid*. **79**, 011801(R) (2009).

[7] G. Steinmeyer, A. Schwache, and F. Mitschke, Phys. Rev. E **53**, 5399 (1996); S. Coen and M. Haelterman, Opt. Lett. **24**, 80 (1999); **26**, 39 (2001).

[8] M. Tlidi, M. Haelterman, and P. Mandel, Europhys. Lett. **42**, 505 (1998); K. Staliunas, Phys. Rev. Lett. **81**, 81 (1998); M. Tlidi, J. Opt. B **2**, 438 (2000); M. Brambilla, T. Maggipinto, G. Patera, and L. Columbo, Phys. Rev. Lett. **93**, 203901 (2004); P. Tassin *et al*., Opt. Express **14**, 9338 (2006); N. Veretenov and M. Tlidi, Phys. Rev. A **80**, 023822 (2009).

[9] A. J. Scroggie, W. J. Firth, G. S. McDonald, M. Tlidi, R. Lefever, and L. A. Lugiato, Chaos Solitons Fractals **4**, 1323 (1994).

[10] F. Leo, S. Coen, P. Kockaert, S.-P. Gorza, P. Emplit, and M. Haelterman, Nat. Photonics **4**, 471 (2010).

[11] S. B. Cavalcanti, J. C. Cressoni, H. R. da Cruz, and A. S. Gouveia-Neto, Phys. Rev. A **43**, 6162 (1991); S. Pitois and G. Millot, Opt. Commun. **226**, 415 (2003); J. D. Harvey, R. Leonhardt, S. Coen, G. Wong, J. C. Knight, W. J. Wadsworth, and P. St. J. Russell, Opt. Lett. **28**, 2225 (2003).

[12] N. Y. Joly, F. G. Omenetto, A. Efimov, A. J. Taylor, J. C. Knight, and P. St. J. Russell, Opt. Commun. **248**, 281 (2005).

[13] A. V. Yulin, D. V. Skryabin, and P. St. J. Russell, Opt. Lett. **29**, 2411 (2004); W. Wadsworth, N. Joly, J. Knight, T. Birks, F. Biancalana, and P. Russell, Opt. Express **12**, 299 (2004); A. Demircan and U. Bandelow, Opt. Commun. **244**, 181 (2005).

[14] J. M. Dudley, G. Genty, and S. Coen, Rev. Mod. Phys. **78**, 1135 (2006); M. Kues, N. Brauckmann, T. Walbaum, P. Groß, and C. Fallnich, Opt. Express **17**, 15827 (2009).

[15] M. Tlidi, A. Mussot, E. Louvergneaux, G. Kozyreff, A. G. Vladimirov, and M. Taki, Opt. Lett. **32**, 662 (2007).

[16] M. Tlidi and L. Gelens, Opt. Lett. **35**, 306 (2010).

[17] T. J. Kippenberg, R. Holzwarth, and S. A. Diddams, Science **332**, 555 (2011); F. Ferdous, H. Miao, D. E. Leaird, K. Srinivasan, J. Wang, L. Chen, L. T. Varghese, and A. M. Weiner, Nat. Photonics **5**, 770 (2011); Y. K. Chembo and C. R. Menyuk, Phys. Rev. A **87**, 053852 (2013).

[18] S. Coen, H. G. Randle, T. Sylvestre, and M. Erkintalo, Opt. Lett. **38**, 37 (2013).

[19] S. Coulibaly, Z. Liu, M. Taki, and G. P. Agrawal, Phys. Rev. A **86**, 033802 (2012); M. Erkintalo, Y. Q. Xu, S. G. Murdoch, J. M. Dudley, and G. Genty, Phys. Rev. Lett. **109**, 223904 (2012); F. Leo, A. Mussot, P. Kockaert, P. Emplit, M. Haelterman, and M. Taki, *ibid*. **110**, 104103 (2013).

[20] G. P. Agrawal, *Nonlinear Fiber Optics*, Optics and Photonics Series, 2nd ed. (Academic Press, San Diego, CA, 1995).

[21] L. A. Lugiato and R. Lefever, Phys. Rev. Lett. **58**, 2209 (1987).

[22] Y. Pomeau, Physica D **23**, 3 (1986).

[23] M. G. Clerc and C. Falcon, Physica A **356**, 48 (2005); U. Bortolozzo, M. G. Clerc, C. Falcon, S. Residori, and R. Rojas, Phys. Rev. Lett. **96**, 214501 (2006); M. G. Clerc, E. Tirapegui, and M. Trejo, *ibid*. **97**, 176102 (2006).

[24] A. Hasegawa and F. D. Tappert, Appl. Phys. Lett. **23**, 171 (1973); **23**, 142 (1973).

[25] L. F. Mollenauer, R. H. Stolen, and J. P. Gordon, Phys. Rev. Lett. **45**, 1095 (1980).

[26] P. Emplit, J. P. Hamaide, F. Reynaud, C. Froehly, and A. Barthelemy, Opt. Commun. **62**, 374 (1987).

[27] S. Coen, M. Tlidi, Ph. Emplit, and M. Haelterman, Phys. Rev. Lett. **83**, 2328 (1999).